Potential of direct solar thermal driven absorption heat pump in hybrid systems

Florian Gritzer[1], Daniel Neyer[1, 2], Manuel Ostheimer [1] and Alexander Thür [1]

[1] University of Innsbruck, 6020 Innsbruck (Austria)

[2] daniel neyer brainworks, 6700 Bludenz (Austria)

Abstract

The energy requirement in buildings is currently changing, the heating demand is decreasing while the cooling demand can be expected to rise. Due to increase of global economics and thus living comfort as well as the need to minimize climate impact highly efficient and renewable solutions for heating and cooling are absolutely essential. Solar thermal and photovoltaic driven systems coupled to thermal/electrical driven heat pumps are promising technologies to satisfy these needs.

However, such systems show a wide range of efficiencies and economics caused by different system designs and control strategies. The research project "SolarHybrid" is systematically processing and optimizing the solar driven systems and their hybrid combinations thereby highly efficient and economic competitive solutions are accomplished.

A study on the hybrid combination of a solar-thermal direct driven absorption heat pump with a vapor compression heat pump for heating and cooling is highlighted here. Up to 80% non-renewable primary energy savings can be realized and despite increased initial investment costs this solution is economic. The results show that levelized energy costs at the same level or even lower as a reference system can be achieved.

Keywords: solar heating and cooling, hybrid systems, solar direct driven absorption chiller

Tab. 1: Nomenclature and Subscripts

ACM	Absorption chiller	HiL	Hardware-in-the-loop	PV	Photovoltaic
C	Cooling	HT	High temperature	Q	Energy [kWh]
CR	Cost ratio (-)	HVAC	Heating, ventilation and air conditioning systems	ref	Reference system
DHW	Domestic hot water	IEA	International Energy Agency	SE	Single effect
ε	Primary Energy Factor (kWh/kWh_{PE})	in	Input	SH	Space heating
EC	Energy Carrier	KPI	Key performance Indicator	SHC	Solar heating and cooling
el	Electrical	loss	Losses	SF	Solar Fraction
equ	Equivalent	LT	Low temperature	SPF	Seasonal Performance Factor (-)
f_{sav}	Savings	NRE	Non-renewable	ST	Solar thermal
η	Efficiency	MT	Medium temperature	sys	System
HB	Hot backup	out	Output	th	Thermal
HE	Half effect	PER	Primary Energy Ratio	VCC	Vapour compression chiller

doi:10.18086/eurosun2018.11.11 Available at http://proceedings.ises.org

1. Introduction

Due to the expected development of the energy demand in the building sector and the global goal to reduce greenhouse gas emissions, the importance of energy-efficient and renewable (solar) heating and cooling systems is increasing. Especially the cooling demand is rising due to growth of global economy and thus increasing living standards (OECD 2018). The consumption of non-renewable primary energy in buildings can be minimized with the implementation of solar driven systems. However, in order to achieve the optimum utilization of non-renewable energy sources the basic energy requirement of buildings must be reduced first. Following this demand optimization, the remaining energy can be covered by solar energy.

The two technologies that are available are solar thermal (ST) or solar-electric (photovoltaic - PV) supported systems. Depending on the boundary conditions, each of the solar technologies offers technical and/or economic advantages compared to standard reference system. However, these two technologies and their technical and economic benefits are still controversial, particularly in the field of heat and cold supply for buildings.

The Austrian "SolarHybrid" research project deals with the systematic processing and optimization of both technologies and their combination for different load profiles. In “SolarHybrid” energy efficient and economic (solar-) hybrid systems for heating and cooling (SHC) are developed. The project includes the development of a NH_3/H_2O single-/half effect absorption chiller (ACM), a NH_3 vapor compression chiller (VCC), their detailed laboratory measurements and system integration as well as comprehensive modelling and system simulations. The systematic validation of the simulation approaches and the individual models including their partial load behavior is an essential basis for modeling. Further investigations are carried out with suitable dynamic simulation models, which are adapted to the laboratory measurements. The solar HVAC systems are adapted and evaluated for three different profiles (office building, hotel and a potential study).

The major barrier to introduce SHC systems in the market are the initial investment costs. To address this barrier, one focus of the project was the reduction of size and number of components. The approach to reduce the system components was (i) to define possible system configurations, (ii) to investigate them in software simulations, (iii) to test both main components (ACM/VCC) in Hardware-in-the-Loop (HiL) tests, (iv) to validate the simulations with the measured data and run annually simulation studies and (v) to assess the results from a technical and economical point of view. The systems are analyzed and evaluated with the standardized evaluation procedure, developed in IEA SHC Task 53 (T53E^4-Tool) (Neyer et al., 2016). This tool is used to evaluate both the technical and the economic potential. The effect of changing technical and economic boundary conditions on key performance indicators (KPIs) are determined with comprehensive sensitivity analyses.

Two chillers/heat pumps were built for the project and optimized for hybrid operation: (i) a vapour compression chiller and (ii) an absorption chiller. The ammonia/water ACM developed in the DAKTris (2013) research project has been further optimized in the SolarHybrid research project and was operated in hybrid operation with the ammonia VCC in hardware-in-the-loop laboratory measurements.

A detailed examination of the components and systems, their modelling and the various load profiles was carried out. The systematic analysis of the simulation approaches and the individual models with their partial load behaviour and their limits of use were the main basis for the following modelling. Dynamic system simulation models are created by selecting and adapting the individual models. Further investigations on system level are carried out accordingly. The hybrid systems were optimized regarding non-renewable primary energy savings with respect to economic benefits. The economic and energetic optimization of solar thermal concepts is achieved by means of three strategies: (i) through adapted hydraulic design, (ii) radically reduced number of components and (iii) improved, more efficient control strategies.

The focus of this paper is on the results of the potential study of the hybrid ACM and VCC operation, which are developed on the basis of laboratory measurements and simulations. This study sought to assess both the technical and economic potential. The potential in maximum supply is evaluated in terms of various temperature levels and applications.

The potential study presented here is showing the potential in terms of minimized and reduced number of components (solar direct fired) and on the other hand the potential of the maximum deliverable energy for given temperature levels.

2. Evaluation

Three methodologies were used to assess the potential of the hybrid ACM and VCC operation. The assessment follows the IEA SHC Task 53 approach and is based on Hardware- in-the-Loop measurements of the single components as well as the hybrid operation and TRNSYS simulations. In this chapter the key performance indicators, the steady state and dynamic laboratory measurements, and the simulation models are discussed. Fig. 1 shows the overall methodological approach of the project. The common nomenclature and subscripts are listed in Tab. 1.

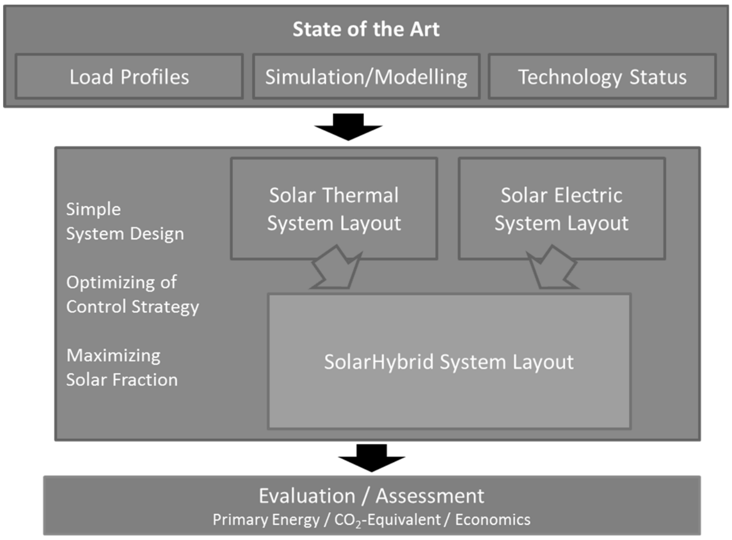

Fig. 1: Methodological approach and workflow of the project SolarHybrid

2.1 Assessment – T53E^4-Tool

In general, the performance evaluation of SHC systems can be complex and the KPIs can be determined in different ways for different boundaries. Thus, the evaluation is carried on technical, economic and ecological aspects according to the methods developed in the IEA SHC Task 48 and 53. The method was implemented in a tool (T53E4 Tool) that contains a database with primary energy factors (ε), efficiencies and economic data for all main SHC components. The evaluation is based on monthly energy balances and includes the calculation of different key performance indicators. The performance evaluation of the SHC system considers the energy distribution in different subsystems for different applications like space heating (SH), domestic hot water (DHW, water heating) and cooling (C).

The most important key figures are explained briefly below. The corresponding equations are shown in Tab. 2. The key performance indicators are defined and discussed in detail by Neyer et al. (2016).

- Non-renewable Primary Energy Ratio (PER_{NRE})

The evaluation is carried out based on non-renewable primary energy (NRE). The PER_{NRE} quantifies the non-renewable primary energy efficiency of the system (eq. 1). The primary energy factors (ε) required for the conversion are depending on type of energy, the location of the system and the season.

- Non-renewable primary energy savings ($f_{sav.NRE}$)

The primary energy of the entire SHC system is compared to a reference system. The standardized Task 53 reference system is an air-cooled compression chiller (VCC) and a natural gas boiler and its primary energy ratio $PER_{NRE.ref}$ is calculated according to eq. 2. Applying both PERs (SHC and ref) the savings can be calculated according to eq. 3.

- Seasonal Performance Factor (SPF)

The SPF is the ratio of useful energy (out: energy supplied to satisfy the needs of the building) to consumed energy from external sources (eq. 4). It is distinguished between thermal and electrical performance.

- Cost Ratio (CR)

The cost ratio is determined with the annualized costs for the SHC system ($C_{use.SHC}$) and the costs for the reference system ($C_{use.REF}$) according to the eq. 5. The annualized costs include investment, replacement, maintenance, electricity, energy, water as well as feed-in tariffs for electricity of photovoltaic etc. The costs are discounted according to the annuity method and are summed up on a yearly basis. If the CR equals one cost parity is reached for the SHC system compared to the defined reference system.

Tab. 2: Overview technical and economic key performance figures defined in IEA SHC Task 53

Non-renewable Primary Energy Ratio	$PER_{NRE} = \frac{\sum Q_{out}}{\sum\left(\frac{Q_{el,in}}{\varepsilon_{el}} + \frac{Q_{in}}{\varepsilon_{in}}\right)}$	(eq. 1)
	$PER_{NRE.ref} = \frac{\sum Q_{out}}{\sum\left(\frac{Q_{out.heat}+Q_{loss.ref}}{\varepsilon_{in}*\eta_{HB.ref}} + \frac{Q_{out.cold}}{SPF_{C.ref}*\varepsilon_{el}} + \frac{Q_{el,ref}}{\varepsilon_{el}}\right)}$	(eq. 2)
Non-renewable Primary Energy Savings	$f_{sav.NRE} = 1 - \frac{PER_{NRE.ref}}{PER_{NRE.sys}}$	(eq. 3)
Seasonal Performance Factor	$SPF_{th} = \frac{\sum Q_{out}}{\sum Q_{in}},\ SPF_{el} = \frac{\sum Q_{out}}{\sum Q_{el,in}}$	(eq. 4)
Cost Ratio	$CR = \frac{C_{use,SHC}}{C_{use,REF}}$	(eq. 5)

2.2 Measurements & Hardware-in-the-Loop

Two tested components are built and optimized in the course of the project. The functional models of an ammonia/water (NH3/H2O) absorption chiller (ACM) and an ammonia vapour compression chiller (VCC) are investigated accordingly. The ACM was developed in the research project DAKTris (2013), it has a nominal cooling power of 20 kW and offers the possibility to switch from single- to half-effect (SE/HE). This enables the possibility of high heat rejection temperatures (up to 45°C), the use of a dry cooling tower and the possibility of high useful temperatures in heat pump-mode. Within this project, the ACM is adapted and optimized concerning the findings in DAKTris and the requirements of SolarHybrid (for example automation of the solvent compensation). In consideration of the hybrid operation the cooling capacity of the VCC is also 20 kW (at nominal condition of evaporation temperature 4°C and condensing temperature 50°C). The main components of the vapour compression chiller are a frequency-controlled piston compressor, a flooded evaporator and a hot gas bypass.

In a first step steady state performance of both machines is measured and characteristic curve diagrams are generated. The second step includes dynamic Hardware-in-the-loop (HiL) tests of the single components and the hybrid operation. The components in the laboratory are integrated in the simulated overall systems (HiL).

- Steady state measurements

Steady state measurements are used to identify the performance at constant operation points. The settings are adjusted accordingly considering the settling time and the measurement period to calculate a representative mean value and the corresponding deviation.

- Dynamic measurements

Based on the stationary results (limiting boundary conditions) and defined system configurations (c.f. next paragraph) a simulation model is set up in TRNSYS. Each configuration is measured under the boundary conditions of two significant days (one sunny, one cloudy) at the chosen location in different variations (temperatures, mass flows, control strategies, SE/HE mode, etc.).

- System configurations

As a consequence, to the idea of minimized and reduced number of components the measured configurations are defined accordingly as direct solar thermal driven systems (no hot water storage). The climatic conditions are simulated for different locations (Innsbruck, Seville, etc.). The solar collector field, the cooling tower and the other components are designed accordingly. The grid provides the required electrical energy.

a) Chiller-mode ACM and VCC: The generator (HT) circuit of the ACM is directly connected to a solar collector field (ST), heat rejection (MT) circuits of both machines are connected in parallel with a dry cooling tower. The chilled water (LT) inlet of the VCC is connected in serial to the outlet of the ACM. Thus, the ACM is cooling the (LT) outlet further down to the required temperature for the cooling load if the power of the ACM is too low. The necessary electricity is drawn from the grid.

b) Heat pump-mode ACM (SE and HE): HT circuit of ACM is directly connected to the collector; MT mass flow is controlled to reach the desired temperature at the MT outlet (useful hot water temperature) of the ACM and the chilled water could be used optionally.

c) Combined chiller- and heat pump-mode ACM and VCC: HT circuit of ACM is directly connected to the collector field, MT and LT circuits of the VCC are connected in serial to the ACM, MT mass flow is controlled to deliver the defined temperature and VCC power is controlled to reach the set LT outlet temperature.

Fig. 2 shows the configuration for the configurations a) and c) on the left side and the configuration b) on the right side.

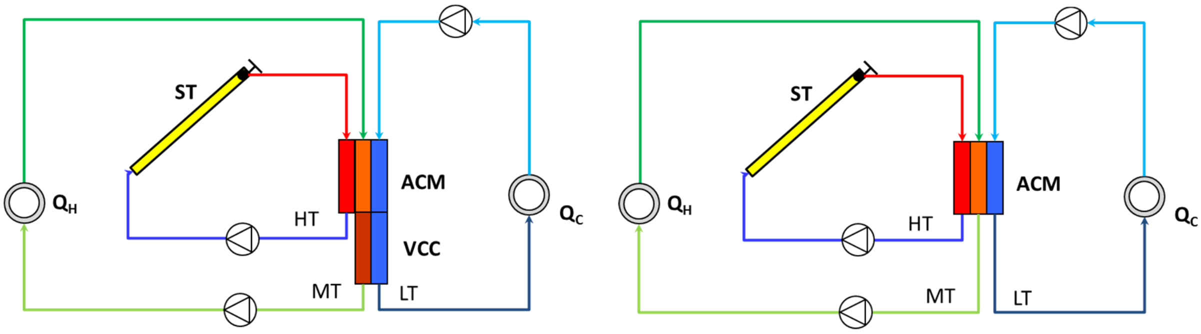

Fig. 2: heat pump and cooling-mode with ACM and VCC (left) and heat pump-mode with ACM only (right)

The main purpose of the combined chiller and heat pump-mode of ACM and VCC (configuration c) is the supply of heat and the simultaneous allocation of cooling energy. The defined temperature levels are 12/6°C for chilled water (LT) circuit, for useful heat of the rejection (MT) circuit 14/40°C and according to the direct coupled solar collector a variable generator (HT) input (60~95°C). The ACM delivers as much as possible (depends on solar irradiation and the reached generator temperature) and the VCC is complementing to deliver the set LT and MT outlet temperature.

Subsequent to the measurements, the evaluated data and energy balances are used to fit the simulation model. Annual simulation studies are carried out for different systems and boundary conditions.

2.3 Simulation studies

The individual models (ACM, VCC, cooling tower, etc.) have been investigated and improved with respect to their partial load behaviour. The ACM and VCC are built up as characteristic curve models and are adjusted to the measured steady state and dynamic data.

The ACM model (Type 1005, Neyer et al., 2015) is based on semi-physical models of a single-effect (SE) ACM (Hannl et al., 2012) and a half-effect (HE) ACM (Zotter et al., 2015). The model can switch between the two operating modes (SE/HE) and its nominal capacity is scalable. A new characteristic curve model has been developed for the VCC. It's also based on a semi-physical simulation model (Luger 2017) that was fitted to the measurements accordingly. The deviation between the simulated and measured daily energy balances for each model is smaller than 3%.

In general, two methods were used to deal with the entire load profiles (heating, cooling, domestic hot water and electricity requirements). The first approach (for a hotel and office building) is using building simulations of the load profiles, the HVAC system is designed according to these load profiles. The second approach used for the potential studies is a reversed way. The HVAC system is designed for a certain capacity (here 20 kW) and is driven by solar only at certain useful temperature levels, thus delivering the maximum possible energy. The real application will either reduce the energy allocated and limiting the technical and economic performance or if the system is applied as base load the sub-system performance keeps the same but the total system performance indicators will change accordingly.

In this paper the results of the potential study are shown only, results of the combined building-HVAC simulations can be found in the final report of the project. The following variants are considered at different temperature levels, control strategies and climatic conditions.

The potentials of the solar directly driven absorption chiller (thermal) are investigated in HiL measurements as well as with simulation studies. The potential studies are carried out for three concepts for heating and cooling (c.f. Tab. 3) resulting in different solar fractions. If the ACM or AHP is operated only, the result is solar fraction 100%. If the output of the VCC/HP is controlled to a certain set outlet temperature via its compressor speed (55-100%), values of approximately 50% are obtained. At maximum compressor speed of the VCC/HP (thus maximum cooling generation) a SF of approximately 35% is achieved.

(i) exclusively solar thermal driven resulting in solar fraction of 100 % (SF 100)

(ii) the hybrid concept, with a controlled operation of the vapor compression chiller (SF 50%)

(iii) the hybrid concept, with maximum chiller/heat pump capacity (SF 37%)

The absorption chiller is directly solar driven, no hot water storage is included. Due to the design of the system the collector can deliver sufficient generator power to run the ACM as soon as the solar irradiation is greater than 200 W/m². To determine the maximum potential of the system for heating, the chilled water circuit (LT circuit) is operated with constant inlet temperature and constant mass flow (simplified control, because there is no constant outlet temperature). The MT circuit is operated with a constant inlet temperature but with a variable mass flow so that a constant outlet temperature is achieved (energy for heating). The MT outlet temperature is controlled to reach 32°C, 40°C, 45°C or 60°C depending on the variation. The AHP is operated in single and half effect (SE/HE). If heating and cooling is investigated in parallel the LT circuit is also controlled to reach the entire set-point.

Tab. 3: Evaluated variants of the potential study and their most important boundary conditions (operation of the ACM/AHP or VCC/HP)

Operating mode	SF 37%	SF 50%	SF 100%
Cooling	ACM + ST direct VCC maximum	ACM + ST direct VCC controlled	ACM + ST direct
Heating	AHP + ST direct HP maximum	AHP + ST direct HP controlled	AHP + ST direct

Selected boundaries for this paper and configuration (c) are presented in Tab. 4. Three operation modes are analysed in order to reach different solar fractions: the ACM in single operation (without LT outlet temperature set point), the ACM with controlled VCC support (to reach the set LT temperature) and the ACM with maximum capacity VCC. The MT inlet temperature (returned to the chiller) is kept constant at 14°C and controlled to reach 40°C outlet (useful) temperature. The LT inlet is kept constant at 12°C The measurements/simulations are executed for the location of Innsbruck and Seville and are distinguished between the use of MT only and the simultaneous MT and LT usage.

Tab. 4: matrix of boundary conditions of the annual simulation for configuration (c)

Use	Location	LT return	MT temp	LT set temp.	Operation mode
MT MT+LT	Innsbruck Seville	12°C	14/40°C	Free floating	ACM only
				6°C	ACM + VCC controlled
				Free floating	ACM + max VCC

3. Results

This paper only shows selected results, more details can be found in the final report of the project SolarHybrid (2014). The steady state results of both chillers as well as the annual simulation results of the above described boundaries are presented in the following paragraphs.

3.1 Component results

According to a defined measurement matrix, steady state measurements of ACM and VCC are executed. The performance maps of ACM (left) and VCC (right) are shown in Fig. 3.

The LT inlet temperature is held at 12°C for both cases (left ACM, right VCC). The MT volume flow rate is held constant at 6.5 m_3/h, LT volume flow is 3 m^3/h for the ACM and 3.5 m^3/h for the VCC measurements. The upper diagram of the ACM map shows the LT capacity over the MT inlet (MT_{in}) temperature and the lower diagram the Energy Efficiency Ratio (EERth) in dependence on MT_{in}. The different lines represent different modes (SE/HE) and different HT inlet temperatures. In SE mode heat rejection temperatures up to 35°C are possible; HE modes enables heat rejection up to 45°C, but at nearly half EER (caused by double generator power). In terms of maximum reachable capacity, switching from SE to HE could be reasonable at a MT inlet temperature higher 32°C (cf. Fig. 3 left, upper diagram).

The VCC map shows the relative performance at a certain part load ratio. The entire performance is compared to that at 100% capacity. The lines represent different MT inlet temperatures, the capacity is first reduced by controlling the compressor speed (100, 75, 50% – right three points of each line) and second through opening a hot gas bypass (left three points of each line). Due to better heat transfer in condenser and evaporator, the maximum EER of the VCC is reached at minimal rpm with closed hot gas bypass.

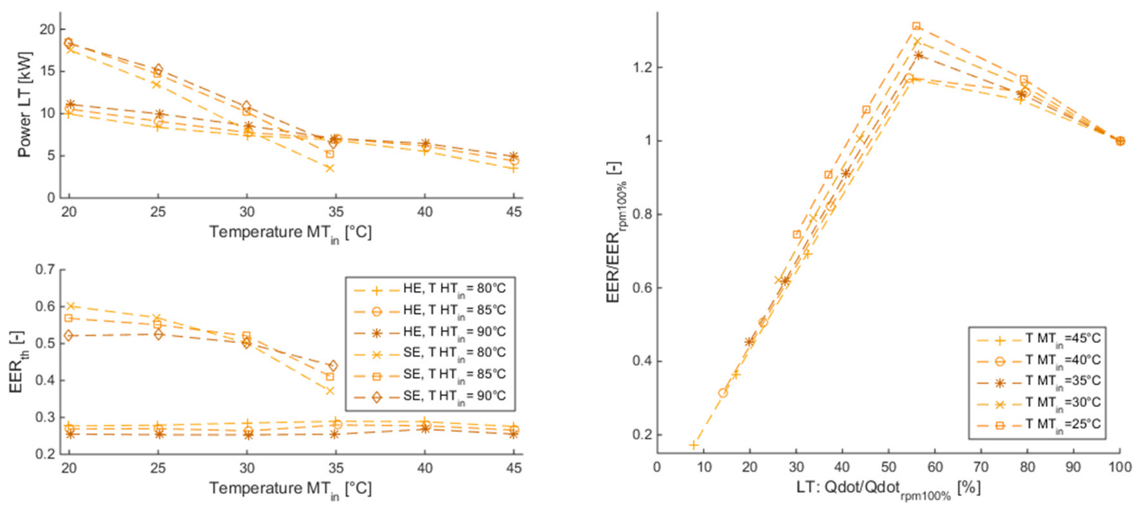

Fig. 3: Performance maps of ACM (left) and VCC (right), LT_{in}=12°C, $\dot{V}_{MT}$=6.5 m³/h, $\dot{V}_{LT.ACM}$=3 m³/h and $\dot{V}_{LT.VCC}$=3.5 m³/h

Both chillers show a good performance, especially under consideration of their status as function models. The further development of the ACM show the expected impact and improve the performance significant. The VCC show EERs far above average (small-scaled chillers) and enables control strategies over a wide range of capacity.

Following the results of one dynamic HiL measurement of the described configuration (c) – combined chiller and heat pump mode of ACM and VCC – are discussed. The results are shown in diagrams, energies are summed up and characteristic performance indicators (e.g. electrical/thermal seasonal performance factor – SPF) are calculated.

Fig. 4 shows the course of a cloudy day (Innsbruck); upper diagram shows the capacities (HT, MT, LT, electrical) of ACM and VCC and the irradiation (multiplied with factor 10) on the collector field; lower diagram shows the corresponding temperatures (MT, LT in- and outlets; HT inlet temperatures multiplied with factor 0.1; ambient temperature)

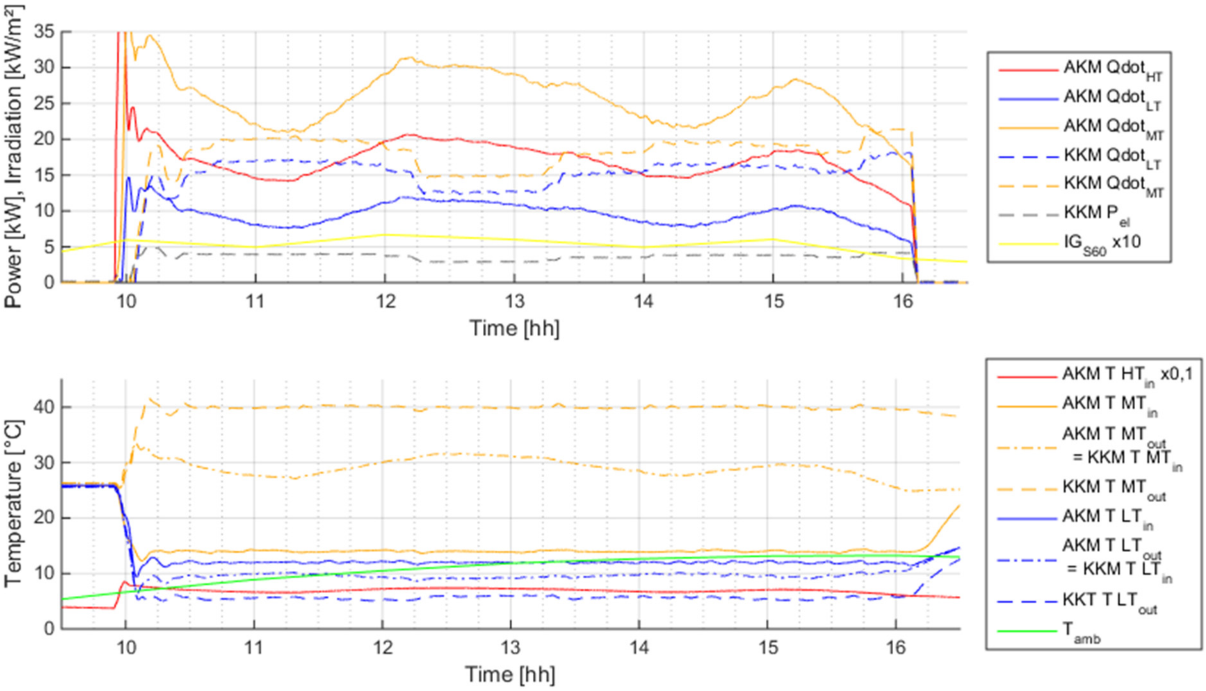

Fig. 4: Combined chiller and heat pump mode of ACM and VCC – course over a cloudy day for Innsbruck climate (upper diagram: power and irradiation; lower diagram: temperatures)

The curves of capacity evolution show the correlation between ACM and VCC, as soon as the ACM delivers less power the VCC raises the power to reach the set point. This results in a constant LT outlet temperature (cf. lower diagram), constant MT outlet temperature is reached by means of controlling MT mass flow.

Tab. 5 shows the energy balances and system SPFs over the daily courses (sunny and cloudy day). The SPFs are distinguished in used energy (MT or MT+LT); the thermal SPF (SPF_{th}) represents the ratio of delivered energy (MT, MT+LT) to used thermal energy (HT); SPF_{el} (electrical) shows the ratio of delivered energy to electrical energy (all circuit pumps, ACM solvent pump, VCC compressor; only compressor measure, pumps).

Tab. 5: Energy balances and SPFs of combined chiller and heat pump mode of ACM and VCC for Innsbruck climate

	Energies ACM [kWh]			**Energies VCC** [kWh]			**ACM+VCC** [kWh]		**System SPF [-]**			
									MT+LT		**MT**	
	Q_{HT}	Q_{LT}	Q_{MT}	Q_{MT}	Q_{LT}	Q_{el}	Q_{MT}	Q_{LT}	SPF_{th}	SPF_{el}	SPF_{th}	SPF_{el}
sunny day	233	125	349	96	80	21	445	205	2,03	20,19	1,50	13,82
cloudy day	102	57	152	102	86	21	254	143	2,04	12,33	1,49	7,89

The configuration with the ACM and VCC used as heat pump reaches in all cases electrical efficiencies of >8. The difference between sunny and cloudy day get obvious but still provide optimization potential as the pumps are all calculated with constant power drawn, including further speed-controlled auxiliaries enables systems with electrical performance of SPF > 10.

3.2 Annual simulation results

Fig. 5 and 6 are showing the annual simulation results of the cooling mode with ACM and VCC and the heat pump mode for this configuration. The three markers for each curve result from pure solar operation (SF = 100%), the controlled combination (ACM+VCC) or the maximum operation of both components (c.f. Tab. 3 & 4)

Both diagrams are comparing the non-renewable primary energy savings ($f_{sav.NRE}$ on x-Axis) to the Cost Ratio (CR on y- axis in reversed order). The less non-renewable primary energy is used the larger the $f_{sav.NRE}$ and thus the results is displayed more on the right end of the diagram. If the annualized cost the solar driven system are lower than those of the reference system the CR results in values lower one and thus results are displayed on the upper end of the diagram.

- cooling-mode

Fig. 5 shows the results for the locations Innsbruck and Seville at two different LT inlet temperatures (the outlet depends on the operating mode). In the diagram, the locations are marked with the same symbols and the temperatures with the same color. In cooling-mode, only the ACM solar thermal direct operation or the hybrid operation of ACM + VCC is analyzed.

The selected system configuration results in maximum savings of non-renewable primary energy savings of 80 to 85%. Although these variations represent 100% solar fraction the savings are lower as the electricity auxiliary demand of the system is considered accordingly. A further optimization of non-renewable primary energy savings could be feasible, but attention must be paid to the ratio of provided (usable) cooling to electrical system efficiency. The $f_{sav.NRE}$ could be further increased at the expense of the CR by a larger design of the solar thermal system (here 3.5 m^2/kW cooling) as well as a larger capacity of the ACM.

The variants with the 12°C LT-return temperatures give a wide spread picture with non-renewable primary energy savings (40 - 80%) and higher CR than with the 22°C variants. The 22°C (LT-return) variants show a steeper and more compact course. This is mainly due to the performance of the VCC, as it operates much more efficiently at higher LT temperatures (rising EER). This results in significantly increased non-renewable primary energy savings (approximately +20% $f_{sav.NRE}$) and additional yield compared to the 12°C variant, which has a positive effect on the cost ratio (CR – 0,1). The markers of the variants with 100% solar fraction (right) at the same location show that the influence of the LT temperature on the performance of the ACM is significantly lower than on the VCC.

The difference between Seville and Innsbruck is obvious. In Seville, higher solar fraction can be achieved due to the larger irradiation with the same configuration compared to Innsbruck. The cost ratio in Seville is correspondingly lower than in Innsbruck. The additional solar yield can be seen in the SF 100% variants; the results for Seville are lower cost ratios (more energy delivered) at slightly lower savings (higher heat rejection temperatures). The results in hybrid operation present the same behavior. Due to the lower performance of the system due to higher heat rejection temperatures the non-renewable primary energy savings are smaller for Sevilla. Due to larger energy provided by the system the CostRatio is decreasing.

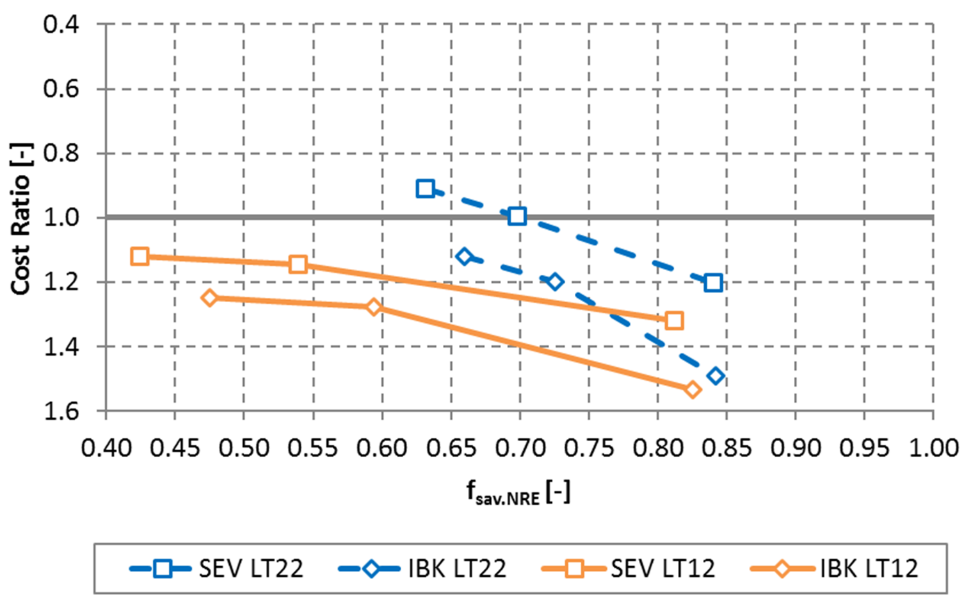

Fig. 5: Comparison of the simulation results for Seville (SEV) and Innsbruck (IBK) for the cooling-mode with 12/6°C and 22/6°C cold water (evaporator) and 14/40°C hot water (condenser) temperature; nomenclature: use(LT) Location LT return, MT in/out

- Heat pump-mode

When switching from pure cooling operation to heat pump operation, the results shown in Fig. 6 are obtained. This figure shows the results for the two locations with pure heat pump operation (MT outlet at 40°C useful temperature) or combined operation with additional chilled water output (LT outlet 6°C).

If both sides of the heat pump can be used, lower levelized costs of energy and CRs and higher non-renewable primary energy savings will result (see diagram on the left). The difference in CR is much more significant with the 100% solar variants than with hybrid use. Although the $f_{sav.NRE}$, which is already > 95%, can hardly be increased any more, the costs are considerably reduced due to the large proportion of MT energy. At the Innsbruck location the CR decreases from approximately 1.4 to 0.8 and in Seville from approximately 0.8 to 0.45, which corresponds approximately (due to the energy balance of ACM) to a multiplication by the EER (~0,6). Also, for the hybrid variations, the CR is reduced by approximately 0.2, with a simultaneous improvement of the $f_{sav.NRE}$ by approximately 5% points.

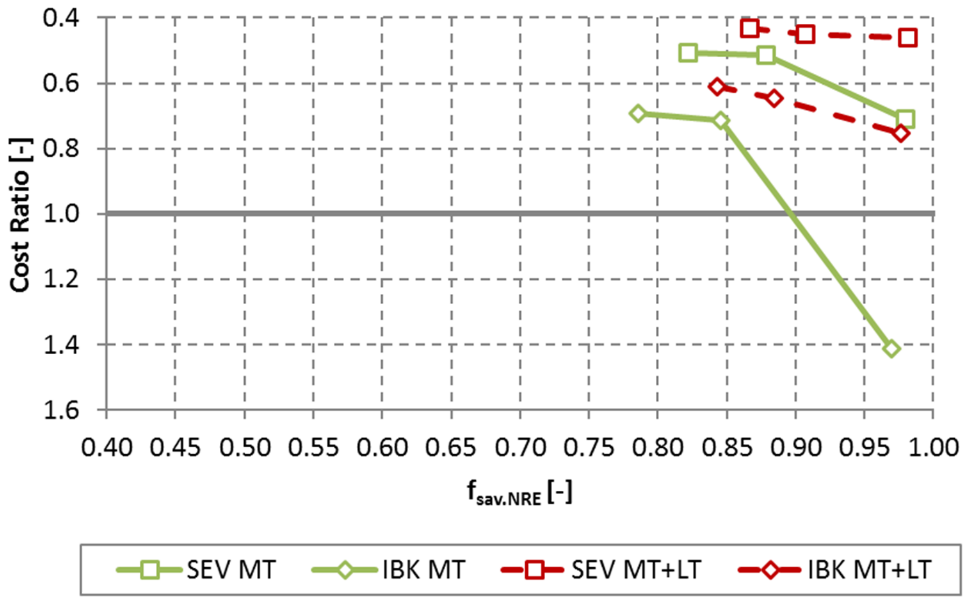

Fig. 6: Comparison of the simulation results for Seville (SEV) and Innsbruck (IBK) for the heat pump-mode with 12/6°C cold water (evaporator) and 14/40°C hot water (condenser) temperature; nomenclature: use(MT, MT+LT) Location LT return, MT in/out

Summing up the potential study illustrates that non-renewable primary energy savings >80% and CostRatio's mostly below 0,8 and as far as 0,4 can be reached by a purely solar driven system. The economic performance is investment cost dominated, thus a sensitivity analysis on different parameters was performed in course of the project but is presented here.

The $f_{sav.NRE}$ are higher with 100% solar thermal systems and with heating operation higher savings can be achieved than with cooling-operation. If both sides of the heat pump can be used (MT&LT) lower cost ratios and higher $f_{sav.NRE}$ can be reached. If the vapour compression system is supporting less (SF 50, SF 100%) the CRs are rising but higher non-renewable primary energy savings can be achieved.

Although the hybrid system with its two heat pumps (chillers) leads to roughly double of investment costs, the CR is lower than with the solar-only operated absorber. With hybrid systems CR lower than one can be achieved. This shows that hybrid systems can be economic viable in comparison with reference systems either for cooling or heating operation.

4. Summary & Conclusion

In SolarHybrid solar heating and cooling systems were investigated intensively by means of simulations, measurements of prototypes and the assessment & benchmarking against conventional system and other solar solutions. All in all, this potential study shows a very interesting starting point for the development of highly efficient and economic solar driven HVAC systems.

- Solar heating and cooling can become cost competitive when systems are designed clever with simple HVAC layouts, advanced control strategies and high efficient components.
- If the load has a cooling requirement, the investigated hybrid cooling systems are cost competitive in regions with higher solar radiation and with 22°C LT temperature. They provide up to 70% non-renewable energy savings
- Non-renewable energy savings can be increased with a larger solar thermal system and more capacity of the absorber but leading to higher Cost Ratios. The focus should be on the reduction of investment costs.

5. Acknowledgment

The contents of this article refer to the SolarHybrid project, developed jointly by the University of Innsbruck, FH OÖ Forschungs und Entwicklungs GmbH, Engie Kältetechnik GmbH and Pink GmbH. The project is funded by the Austrian Climate and Energy Fund and is a part of the Energy Research Program 2013.

6. References

DAKTris, 2013: Dynamisches Betriebsverhalten von AKM im gebäudeübergreifenden TRI-Generation Betrieb (FFG Projekt Nr. 840650). Wien: Österreichische Förschungsförderungsgesellschaft - FFG.

Hannl, D., Rieberer, R., 2012. Analyse einer Ammoniak/Wasser Absorptionskälteanlage – Betriebserfahrungen okund Simulationsmodellbildung, DKV-Tagung 2012, Würzburg

Luger, Stefan: Giovanni, Aldo: (2017) Analyse einer Kompressionskältemaschine zur Kaltwassererzeugung mit kleiner Leistung im überfluteten Thermosiphonbetrieb mit Drehzahl- und Heißgasbypass- Leistungsregulierung mit dem natürlichen Kältemittel Ammoniak, Bachelorarbeit am MCI Innsbruck, Juli 2017

Neyer, D.; Thür, A.; Neyer, J.; Zotter, G.; Rieberer, R.; Pink, W.; Halmdienst, C., (2015) Operating Conditions of a NH3/H2O Chiller for Tri-Generation Systems – Chiller Adaption and First Results. SAC 2015, Rom

Neyer D., Neyer J., Stadler K., Thür A., (2016). Deliverable C3-1: TASK 53 - Energy-Economy-Ecology-Evaluation Tool T53E4-Tool, Tool Description and introductory Manual, SHC Task 53

OECD/IEA (2018): The Future of Cooling. Opportunities for energy efficient air conditioning. Hg. v. IEA Publications, International Energy Agency.

SolarHybrid, 2014. Solare Hybridsysteme zum Heizen und Kühlen - Mit Optimierungen zu minimierten und kostengünstigen Systemkonzepten, Energy Mission Austra, e!Mission 2013, FFG Nr. 843855, Vienna, Austria

Zotter, G. et al.,(2015) Optimierung einer Ammoniak/Wasser-Absorptionskältemaschine für Kraft-Wärme-Kältekopplungen auf Basis von BHKWs kleiner Leistung, Dresden, Deutscher Kaelte- und Klimatechischer Verein (DKV)